Synthesis, Self-Assembly Properties, and Degradation Characterization of a Nonionic Photocleavable Azo-Sulfide Surfactant Family

Kyle A. Brown,*,[#] Morgan K. Gugger,[#] David S. Roberts, David Moreno, Pil Seok Chae, Ying Ge, and Song Jin*

Read Online

ACCESS | Metrics & More | Article Recommendations | Supporting Information

ABSTRACT: We report the synthesis and characterization of a new family of maltose-derived nonionic surfactants that contain a photocleavable azo-sulfide linker (mAzo). The self-assembly properties of these surfactants were investigated using surface tension measurements to determine the critical micelle concentration (CMC), dynamic light scattering (DLS) to reveal the hydrodynamic radius of their self-assemblies, and transmission electron microscopy (TEM) to elucidate the micelle morphology. Ultraviolet−visible (UV−visible) spectroscopy confirmed the rapid photodegradation of these surfactants, but surface tension measurements of the surfactant solutions before and after degradation showed unusual degradation products. The photodegradation process was further studied using online liquid chromatography coupled with mass spectrometry (LC−MS), which revealed that these surfactants can form another photo-stable surfactant post-degradation. Finally, traditionally challenging proteins from heart tissue were solubilized using the mAzo surfactants to demonstrate their potential in biological applications.
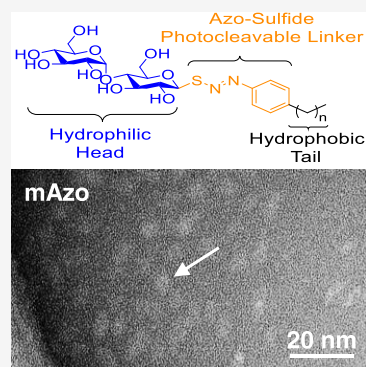
INTRODUCTION

Surfactants are molecules that contain both a hydrophobic and hydrophilic component.[1−3] They can alter the surface tension of the liquid in which they are present and have proven to be valuable across several industries and scientific fields ranging from vessels for chemical reactions to membrane mimics for the characterization of biomolecules.[1−6] Consequently, it is important to develop and characterize new surfactant compounds with specifically desired attributes. Surfactants have been traditionally categorized as ionic, zwitterionic, or nonionic, and these characteristics have important behavioral implications that make the surfactants suitable for different applications. For example, nonionic surfactants can preserve the native states and biological functions of proteins.[7−9] They can also act as effective templates to design and synthesize mesoporous solids, a process termed nonionic-surfactant-templating.[10] More recently, novel surfactants with unique properties, such as cleavable surfactants, multimeric surfactants (*e.g.*, Gemini and trimeric), and surfactants with constituents of biological origin, have been of increasing interest.[11,12]

Cleavable surfactants, wherein a weakened bond is engineered between the hydrophobic and hydrophilic portions of the molecule, can be especially useful when their surface tension-altering property is initially needed yet is a subsequent nuisance. Several cleavable motifs are labile under various external stimuli including light, acid, alkali, temperature, redox environment, and enzymatic conditions.[12−24] Light offers advantages over other stimuli, as it can be administered at a specific time and location within a larger system, it is relatively inexpensive, and it is noninvasive.[25] Some of the most widely used photocleavable motifs include phenacyl, nitrobenzyl-based, azo-based, and benzyl-based.[18,26−29] For example, our lab recently demonstrated the use of an anionic azobenzene photocleavable surfactant (Azo) for protein extraction and subsequent proteomic analysis following rapid surfactant degradation.[13,30−33] However, the ionic nature of Azo surfactant prevents its biological applications where the proteins cannot be denatured. It is desirable to develop new classes of photocleavable surfactants with milder nonionic head and tail groups for a wide variety of biological applications.

Here, we have synthesized and characterized the molecular and supramolecular properties of a novel family of nonionic sugar-derived surfactants containing a photocleavable motif (Figure 1). This surfactant series, which we refer to as mAzo, consists of a hydrophilic head of maltose,[34,35] a photocleavable azo-sulfide linker, and a phenylalkyl hydrophobic tail with alkyl chains ranging between 6 and 10 carbons to explore how the relative hydrophobicity affects aspects of the compounds and
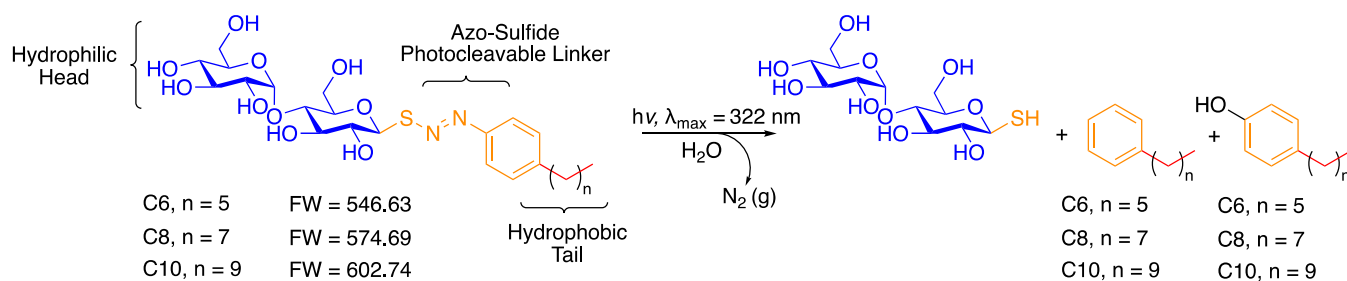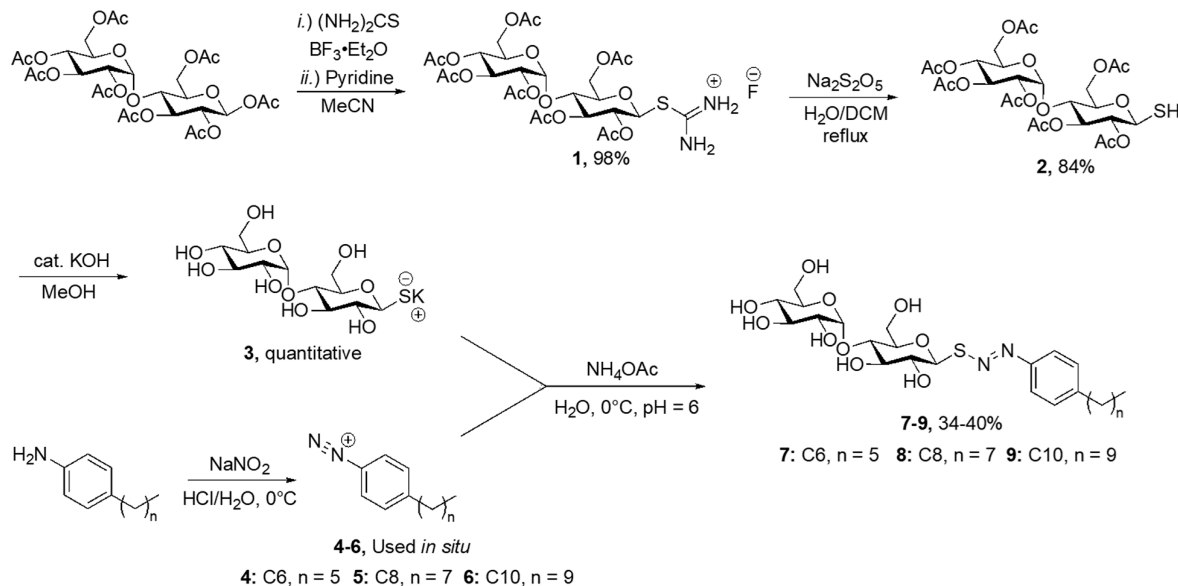
Figure 1. Design of a family of nonionic photocleavable surfactants (mAzo) consisting of a maltose head group, azobenzene linker, and tunable alkyl chain, and the hypothesized photodegradation pathway.

Scheme 1. Synthetic Scheme for the mAzo Surfactant Family

their assemblies. It is expected that, upon ultraviolet (UV) irradiation, the azo-sulfide would homolytically cleave to expel nitrogen gas, leaving behind alkylbenzene and phenolic-derived products as well as thiomaltose based on a previous work on the Azo surfactants (that contain a sulfate head group).[23,26,36] However, detailed characterization of the properties of the surfactant uncovered a secondary degradation pathway leading to the formation of a new surfactant that alters surface tension. These results provide insights into the continued development and application of photocleavable surfactants.

EXPERIMENTAL SECTION

Reagents and Materials. All chemicals and reagents were obtained commercially and used without further purification. The β-D-maltose octaacetate, ammonium acetate (NH$_4$OAc), thiourea, and high-performance liquid chromatography (HPLC)-grade water (H$_2$O) were purchased from Fischer Scientific. Boron trifluoride diethyl etherate (BF$_3$·Et$_2$O), sodium metabisulfite (Na$_2$S$_2$O$_5$), magnesium sulfate (MgSO$_4$), sodium nitrite (NaNO$_2$), hydrochloric acid (HCl), potassium hydroxide (KOH), dichloromethane (DCM), acetonitrile (MeCN), ethyl acetate (EtOAc), anhydrous methanol (MeOH), anhydrous chloroform (CHCl$_3$), and silica were all purchased from Sigma-Aldrich. 4-n-Hexylaniline, 4-n-octylaniline, and 4-n-decylaniline were all obtained from TCI America. Protein extraction solutions were made in nanopure water, ammonium bicarbonate (NH$_4$HCO$_3$), potassium chloride (KCl), sucrose, sodium fluoride (NaF), phenylmethanesulfonyl fluoride (PMSF), L-methionine, ethylenediaminetetraacetic acid (EDTA), and n-dodecyl-β-D-maltoside (DDM) were all purchased from Sigma-Aldrich. Swine

heart tissue was obtained from healthy Yorkshire domestic pigs and had been flash-frozen in liquid N$_2$ and stored at −80 °C prior to use. The Protein Assay Dye Reagent Concentrate was obtained from Bio-Rad.

Surfactant Synthesis. The synthesis of the family of mAzo surfactants followed the multistep process outlined in Scheme 1.

1-Isothiouronium-β-D-maltose Heptaacetate Fluoride (1). Thiourea (0.418 g, 5.50 mmol, 1.10 equiv) was added to a stirring solution of β-D-maltose octaacetate (3.39 g, 5 mmol, 1 equiv) in dry acetonitrile (10.0 mL). Then, BF$_3$·Et$_2$O (1.85 mL, 15.0 mmol, 3 equiv) was added and the reaction was allowed to proceed under reflux for 20 min. All starting material should disappear at this time. The reaction mixture was cooled to room temperature before adding pyridine (15.0 mmol, 1.19 g, 1.21 mL, 3 equiv) and concentrating *in vacuo* to a syrup. The syrup was dissolved in 40 mL of EtOAc and washed with HPLC-grade water (3 × 20 mL). The organic layer was then dried with anhydrous MgSO$_4$ and concentrated *in vacuo*.[37] The isothiouronium salt **1** was obtained as a white amorphous solid and used without further purification. Crude yield, 98%.

1-Thio-β-D-maltose Heptaacetate (2). Sodium metabisulfite (7.50 mmol, 1.43 g, 1.50 equiv), DCM (23 mL), and HPLC-grade water (13 mL) were added to the isothiouronium intermediate **1** (3.51 g, 5.00 mmol, 1.00 equiv), and the reaction mixture was refluxed at ∼60 °C for 3.5 h. After the mixture was cooled to room temperature, the aqueous layer was decanted and extracted with DCM (2 × 20 mL). The organic layers were then recombined and washed with brine (1 × 10 mL), dried over anhydrous MgSO$_4$, and concentrated *in vacuo* to afford **2** as an amorphous white solid, which was used in the following steps without further purification.[38] Yield, 84%.

1-Thio-β-D-maltose Potassium Salt (3). Peracetylated 1-thio-β-D-maltose **2** (1.00 g, 1.53 mmol, 1.00 equiv) was suspended in a

solution of anhydrous MeOH (5 mL) containing KOH (100 mg, 1.78 mmol, 1.18 equiv). The deacetylation was allowed to proceed for 30 min to afford a white precipitate before adding EtOAc (5 mL). The reaction mixture was then centrifuged, and the supernatant was discarded. The solid was washed once more with EtOAc (5 mL), isolated *via* centrifugation, and dried overnight in a desiccator to afford **3** as a white solid in quantitative yield.

4-n-Alkyl Diazonium Chloride Salts (4, 5, 6). 4-*n*-Hexylanilne (C6) (115 mg, 0.649 mmol, 1.0 equiv) was added to a solution of 11 M HCl (215 μL) and HPLC-grade water (630 μL), and the mixture was stirred at 0 °C in an ice bath for 5 min before a cooled solution of NaNO$_2$ (63 mg, 0.914 mmol, 1.4 equiv) in HPLC-grade water (630 μL) was added dropwise over 5 min. The same procedure was scaled and repeated for 4-*n*-octylaniline (C8) (116 mg, 0.568 mmol, 1.0 equiv) and 4-*n*-decylaniline (C10) (35.2 mg, 0.151 mmol, 1.0 equiv). The reaction mixtures were stirred for 20 min at 0 °C to afford clear, colorless to slightly yellow solutions of diazonium chloride salts **4**−**6** in assumed quantitative yields, which were used *in situ* in the following steps.[23]

Maltose Azo-Sulfide Surfactants [7 (mAzo 6), 8 (mAzo 8), 9 (mAzo 10)]. To the stirred solution of diazonium salt **4**, ice-cold NH$_4$OAc (6 M) was added dropwise until a pH of 6 was attained. This buffered solution was then added dropwise to a stirred, cooled solution of **3** (410 mg, 0.965 mmol, 1.7 equiv) in HPLC-grade water (2.0 mL), and a bright yellow product was immediately observed. The same procedure was scaled and repeated for the solutions of **5** and **6**, and supplemental water was added in 200 μL aliquots for ease of stirring. After allowing the reaction to stir for a further 30 min at 0 °C, a volume of chloroform equivalent to the aqueous reaction mixture was added. Methanol was then added in 100 μL aliquots, and the mixture was shaken vigorously until the yellow product was observed to migrate into the organic layer. The organic layer was then removed, dried with anhydrous MgSO$_4$, and the solvent was removed *in vacuo* without applying heat. The crude solids of **7**−**9** were purified by silica flash chromatography using ice-cold solvent (DCM:MeOH 80:20; R_f = 0.3 (C6), R_f = 0.4 (C8), R_f = 0.45 (C10)) to afford **7**−**9** as a bright yellow solid. Yield, 39% (C6), 40% (C8), 34% (C10).

Surfactant Characterization. The mAzo surfactants and the resulting degradation products were characterized using the following methods:

^{1}H NMR. Spectra were recorded on a Bruker Avance-400 MHz spectrometer at room temperature and referenced using residual undeuterated solvent peaks (DMSO-d_6, δ_H = 2.50 ppm; D$_2$O, δ_H = 4.79 ppm). The ^{1}H NMR spectra and associated peak shifts for compounds **1**−**9** are displayed in Figures S1−S6.

Surface Tension Measurements. Critical micelle concentration (CMC) values were obtained using a Tensiometer Kruss K10T equipped with a Wilhelmy plate. A 1% wt solution of **7** (mAzo 6) and **8** (mAzo 8) as well as a 0.1% wt solution of **9** (mAzo 10) was prepared in nanopure water and kept in an ice bath. Small aliquots of each surfactant were added to 10 mL of ice-cold nanopure water under continuous stirring, and surface tension measurements were taken and plotted as a function of the logarithm of their corresponding concentration. The measurements were repeated three times for each surfactant.

Dynamic Light Scattering. Dynamic light scattering (DLS) measurements were carried out using a Malvern Zetasizer Nano ZSP. Solutions were prepared for each surfactant at 30× their measured CMCs in degassed nanopure water. The surfactant solutions were then passed through a 0.2 μm filter and centrifuged at 21,100g for 10 min at 4 °C. Samples were allowed to equilibrate in the zetasizer for 120 s before DLS measurements were taken. DLS experiments were repeated three times on each sample.

TEM Imaging. The surfactants were suspended in nanopure deionized water from Milli-Q water (MilliporeSigma) at 30× their measured CMCs, sonicated for 2 min, and allowed to equilibrate in the dark for 10 min. Transmission electron microscopy (TEM) samples were prepared by mixing surfactant solutions with a 4% wt aqueous phosphotungstic acid solution (pH 7.4) (MilliporeSigma) in a 1:1 ratio by volume, and then one drop of the surfactant solution

was pipetted onto a formvar-coated copper TEM grid with carbon film for negative staining. TEM imaging was conducted on an FEI Tecnai TF 30 TEM instrument operated at 300 kV and equipped with a Gatan K2 direct electron detector for low-dose TEM. Images were collected with a total electron dose of 10 e/Å^2, and all images were processed with digital micrograph software program.

Photodegradation Analysis by UV−Vis. All UV−visible (UV−vis) absorbance measurements were performed on a PerkinElmer Lambda 10 spectrophotometer. A 0.014% wt solution of each surfactant was prepared and aliquoted into 1.5 mL Lo-Bind Eppendorf centrifuge tubes. Samples were then irradiated using a 100 W high-pressure mercury lamp for 0, 30, 120, or 600 s. Samples were then immediately flash-frozen at −80 °C and thawed at 4 °C before taking absorbance spectra.

LC−MS of the Degradation Products of Surfactants. Liquid chromatography−mass spectrometry (LC−MS) was performed on a Waters nanoACQUITY HPLC coupled to a maXis II ETD Q-TOF (Bruker Daltonics). Surfactant or degraded product (2 μg) was loaded onto a home-packed C2 column (500 μM) and separated at room temperature with a flow rate of 12 μL/min using a 35 min gradient from 40 to 95% B with mobile phases of 0.2% formic acid in water (A) and 0.2% formic acid in ACN:IPA (1:1) (B). Compounds eluted from the column were infused and ionized using a capillary voltage of 4500 V and transmitted with an endplate voltage of 500 V. MS scans were collected at 1 Hz from 500 to 2000 *m/z*.

Insoluble Protein Extraction and Bradford Assay. The following protein extraction was carried out at 4 °C. Swine heart tissue (230 mg) was cut into small pieces and homogenized for 1 min in 1 mL of a lysis buffer containing 1 mM EDTA, 25 mM NH$_4$HCO$_3$, 250 mM sucrose, 500 mM KCl, 500 mM NaF, 2 mM L-methionine, and 1 mM PMSF. The homogenate was then centrifuged at 21,100 g for 10 min, and the supernatant was removed and discarded. The tissue pellet was then rehomogenized for 1 min in 1 mL of a washing buffer containing 25 mM NH$_4$HCO$_3$, 2 mM L-methionine, and 1 mM PMSF, centrifuged for 10 min at 21,100 g, and the supernatant was removed. This washing process was repeated twice more, wherein the homogenate from the final wash was first partitioned into 21 separate 1.5 mL Eppendorf centrifuge tubes. To each tissue pellet was then added 100 μL of 25 mM NH$_4$HCO$_3$ containing no surfactant (NS, control), 1.0% wt mAzo 6, 1.0% wt mAzo 8, 1.0% wt mAzo 10, 1.0% wt DDM, 1.0% wt Azo 6, or a maximally concentrated solution of Azo 8. Each of these seven conditions was tested three times. The insoluble pellets were then resuspended, and the extraction was allowed to proceed for 1 h before centrifuging at 21,100g and collecting the supernatant. The concentration of the protein in the supernatants was determined using a Bradford Assay on a small, diluted sample aliquot and measuring the absorbance at 595 nm after a 5 min incubation period.

SDS-PAGE of Extracted Proteins. To 40 μL of each supernatant, 160 μL of ice-cold acetone was added, and the samples were allowed to sit overnight at −20 °C. After the samples were centrifuged for 10 min at 21,100g and the supernatant was removed, the precipitated proteins from each sample were reconstituted in 40 μL of 1× Laemmli buffer, of which 5 μL was loaded into a 1 mm, 10 well 12.5% sodium dodecyl sulfate (SDS) polyacrylamide gel made in-house. Proteins were resolved by applying 70 V for 20 min and subsequently 120 V for approximately 80 min, and the bands were visualized using Coomassie Brilliant Blue.

■ RESULTS AND DISCUSSION

We report the successful synthesis of a new class of photocleavable, nonionic surfactants (mAzo) derived from the maltose hydrophilic head group, azo-sulfide linker, and hydrophobic 4-*n*-alkyl anilines. These mAzo compounds represent novel analogues of the previously characterized alkylbenzene azosulfonates[23,26] but have a highly water-soluble maltose head group. This was chosen to mimic the properties of the commercially available nonionic surfactant DDM, which
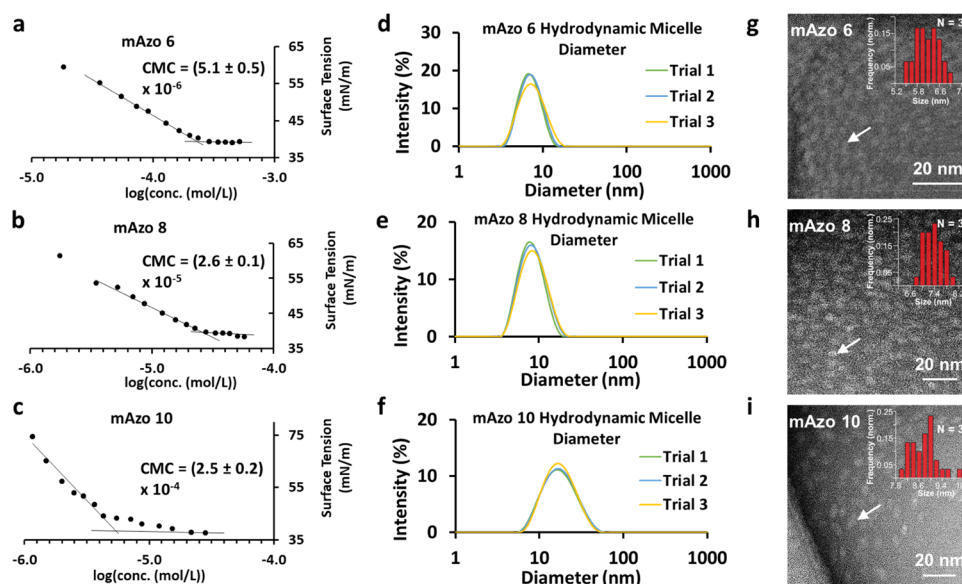
Figure 2. Characterization of the supramolecular assemblies formed by the mAzo surfactants. (a−c) Surface tension measurements at different surfactant concentrations with linear regression fits to decline and plateau regions for mAzo 6, mAzo 8, and mAzo 10. (d−f) Triplicate trial overlay of hydrodynamic micelle diameters for mAzo 6, mAzo 8, and mAzo 10 as measured by DLS. (g−h) Representative low-dose TEM images of mAzo 6, mAzo 8, and mAzo 10 obtained by negative stain contrast showing micellar structures. The insets show the micelle size distribution histograms.

has been widely used in biology for protein purification and crystallography.[7] We envision that additional photodegradable surfactants featuring a variety of head groups (*e.g.*, different sugar moieties, oligoglycerols, *etc.*) could be developed using a similar process described here, which would have unique properties.

The surfactants were synthesized in four total steps (Scheme 1), the first three of which were used to form 1-thio-*β*-D-maltose (**3**). Commercially available peracetylated maltose was first taken to its 1-isothiouronium derivative **1** by exploiting the increased electrophilicity of the sugar's anomeric position, using thiourea as a nucleophile in an S_N2 substitution. The isothiouronium moiety was reduced to thiol **2**, which was then subjected to alkaline deacetylation conditions to afford **3** as a potassium salt. Diazonium salts **4−6** were synthesized in aqueous conditions from 4-*n*-hexylaniline (C6, mAzo 6), 4-*n*-octylaniline (C8, mAzo 8), or 4-*n*-decylaniline (C10, mAzo 10), respectively. The final coupling step between **3** and diazonium salts **4−6** afforded amphiphiles **7** (mAzo 6), **8** (mAzo 8), and **9** (mAzo 10), respectively. At 4 °C, both mAzo 6 and mAzo 8 are soluble at or above 10% wt in nanopure water, whereas mAzo 10 is soluble at up to 2% wt. Successful synthesis was confirmed by NMR spectra of the individual mAzo compounds (Figures S1−S6). A family of surfactants was made using the same approach with a glucose head group; however, they suffered from poor water solubility (<0.5% wt for all).

The solution stability of these new surfactants (**7−9**) was tested using UV absorbance for up to 24 h. The mAzo surfactant solutions in water appear to be unstable when maintained at room temperature in the dark, as the UV−vis absorbance spectra show substantial degradation at 6 h and almost complete degradation by 24 h (Figure S7). The previously studied Azo surfactants were found to be stable in water at room temperature and higher.[13,23] When the mAzo surfactant solutions were stored at 4 °C in the dark, minimal degradation was observed even after 24 h. Due to the labile nature of this surfactant family, the proceeding characterization

experiments were carried out at colder temperatures (4−10 °C) instead of at room temperature. However, thermally labile molecules have been reported to be beneficial in drug delivery and in green chemistry, which both rely on biodegradability; thus, this property could be advantageous in select applications.[39]

The self-assembly of surfactants into structures like micelles or vesicles is a key property of these materials. Micelles are the simplest of amphiphile supramolecular assemblies, and their formation is driven by the hydrophobic effect.[40] We monitored changes in the surface tension as a function of the mAzo surfactant concentration as there is a linear dependency with respect to the logarithm of surfactant concentration until the critical micelle concentration (CMC) is reached, and little or no change is then observed (Figure 2a−c). By averaging three trials of such surface tension measurements (additional results shown in Figure S8), we determined the CMCs to be $(5.1 \pm 0.5) \times 10^{-6}$, $(2.6 \pm 0.1) \times 10^{-5}$, and $(2.5 \pm 0.2) \times 10^{-4}$ mol/L for mAzo 10, mAzo 8, and mAzo 6, respectively. A decrease in CMC with the addition of two carbons on the tail follows the trend observed with the Azo surfactants.[26] For mAzo 10, a slight uncharacteristic decrease in surface tension was observed after the CMC was reached (Figure 2c), which could be caused by impurities (such as a small amount of thermally degraded surfactant, which will be discussed later). Because mAzo 10 has the lowest CMC, it is likely the most affected by any impurity.

Next, we measured the micellar size and size distribution using dynamic light scattering (DLS). Because the measurement is made based on particle diffusion in a fluid, the micellar size measured is referred to as its hydrodynamic diameter.[41] Intensity percentage as a function of the hydrodynamic micelle diameter distributions of mAzo 6 (7 ± 1 nm), mAzo 8 (9 ± 2 nm), and mAzo 10 (19 ± 5 nm) can be seen as a set of three separate trials (Figure 2d−f). Typical hydrodynamic micelle diameters of surfactants are less than 50 nm,[42] and commonly used commercially available nonionic surfactants such as DDM, Triton X-100, and Tween 20 fall at the lower end of this range,[43] as do the values obtained for the mAzo surfactants
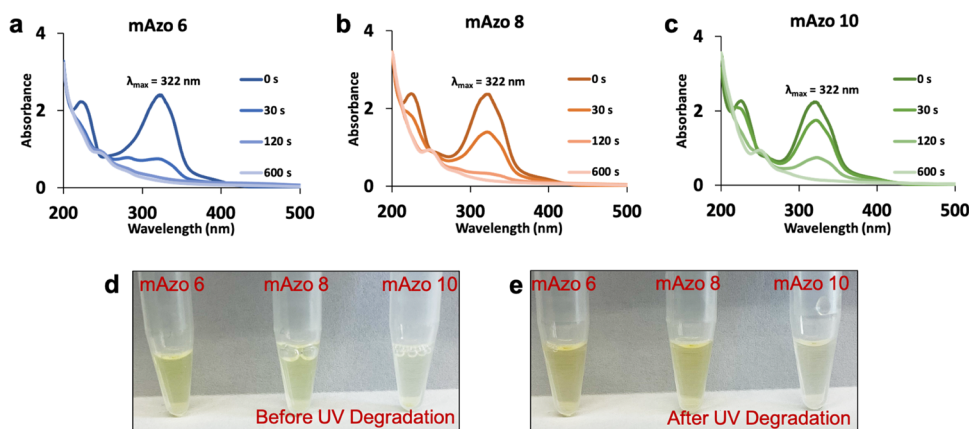
Figure 3. (a−c) UV−visible absorbance spectra for mAzo 6, mAzo 8, and mAzo 10 (0.014% wt, 4 °C) after 0, 30, 120, and 600 s of photoirradiation. (d, e) Photographs of the solutions of mAzo 6, mAzo 8, and mAzo 10 before and after photoirradiation.

(Figure 2d−f). As the aliphatic chain length increases among the mAzo surfactants, the hydrodynamic diameter increases as expected.

Negative stain low-dose TEM imaging was used to further corroborate the size and distribution measurements obtained from DLS, as well as to reveal micellar morphology and other properties. In general, the mAzo surfactant family showed slightly elongated spherical micelle morphologies (Figure 2g−i) with increasing average sizes moving from mAzo 6 (5.8 ± 0.5 nm) to mAzo 8 (7.4 ± 0.7 nm) and to mAzo 10 (9.0 ± 1.0 nm). This increase in TEM average size as a function of increased aliphatic chain length for the mAzo surfactants agrees with the trend of increasing hydrodynamic diameter of mAzo 6 to mAzo 10 observed above in the DLS results.

We next used UV−visible spectroscopy to examine the photodegradation of the mAzo surfactants. For each variant, a $\lambda_{max-abs}$ was observed at 322 nm (Figure 3a−c), and the largest contribution to this absorbance is from the azo chromophore, which also gives these surfactants their characteristic bright yellow hue. Specifically, the electronic transition that takes place to create this absorbance maximum is $\pi_{N=N} \rightarrow \pi^*_{N=N}$, and the absence of this transition can be used to monitor the photodegradation process (Figure 3a−c). This photodegradation can also be visualized when the color changes from bright yellow before degradation (Figure 3d) to slightly darker after degradation (Figure 3e). When comparing across UV−visible absorbance spectra, the degradation time appear to be correlated with the aliphatic chain length. After 120 s, mAzo 6 is completely degraded, whereas mAzo 8 or mAzo 10 takes around 600 s for complete degradation. The second absorbance maximum, corresponding to the aromatic region of the surfactants, also disappears post-photodegradation and is replaced by a smaller band at ~255 nm, congruent with the changes in ring electronics post-degradation.

To further characterize the photodegradation products of the surfactants, we took surface tension measurements of the whole surfactant solutions after photodegradation. A 0.1% solution of each surfactant was irradiated for 10 min and diluted as previously described to perform the series of surface tension measurements. Surprisingly, surface tension still decreased linearly with increasing surfactant concentration (Figure 4), instead of remaining constant around the level of water, as would be expected with the complete destruction of the surfactant. This behavior was unexpected based on the anticipated degradation products (illustrated in Scheme 1)
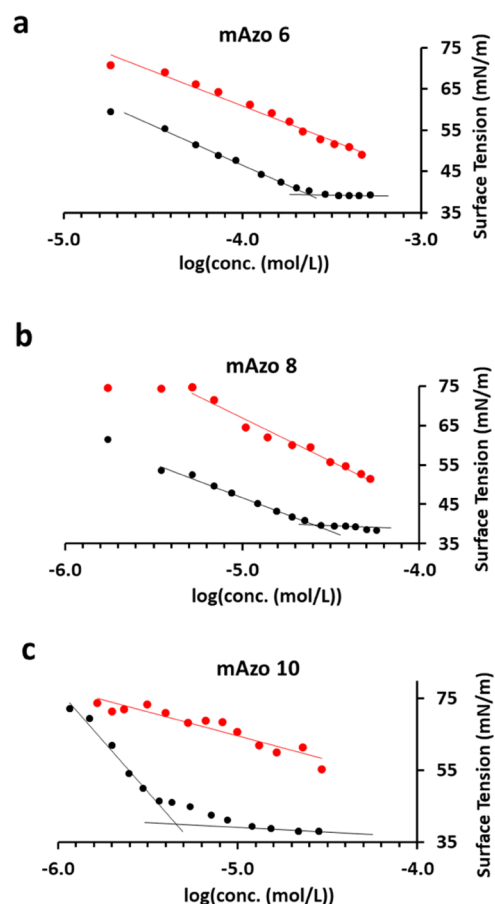

Figure 4. Whole-solution surface tension measurements as a function of surfactant concentration before (black) and after (red) photo-irradiation (10 min) of 0.1% (a) mAzo 6, (b) mAzo 8, and (c) mAzo 10.

because they are not likely to alter surface tension to this extent.[26] Thus, we hypothesize that a new, surfactant-like species could form from the recombination of the hydrophilic and hydrophobic fragments after the photodegradation.

To investigate the surfactant degradation mechanism, we performed liquid chromatography (LC)-MS analysis to identify the photodegradation products, which differ from the previously established photodegradation mechanism of azobenzene-containing surfactants.[26] Before photodegradation,
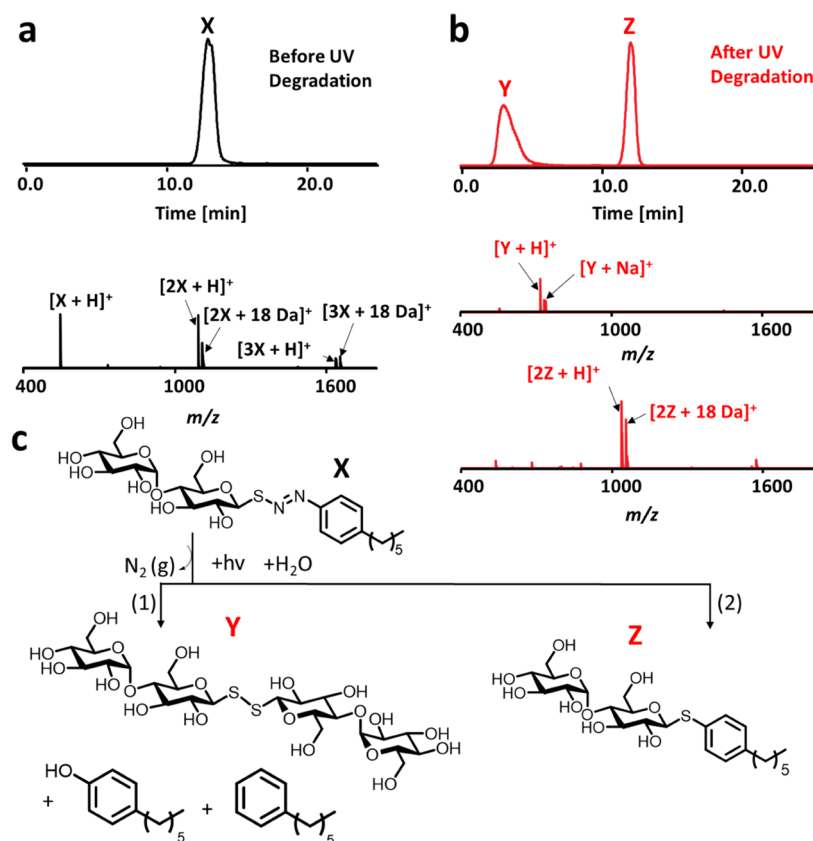
Figure 5. Representative extracted ion chromatograms and the corresponding mass peaks before (a, black) and after (b, red) photoirradiation for mAzo 6 obtained *via* LC−MS. ESI-MS for mAzo 6 ($C_{24}H_{39}N_2O_{10}S$), $[M + H]^+$, calcd m/z: 547.2325, exptl m/z: 547.2300, error: −4.6 ppm. ESI-MS for maltose disulfide ($C_{24}H_{43}O_{20}S_2$), $[M + H]^+$, calcd m/z: 715.1789, exptl m/z: 715.1751, error: −5.3 ppm. ESI-MS for the thioether degradation product ($C_{48}H_{77}O_{20}S_2$), $[2M + H]^+$, calcd m/z: 1037.4450, exptl m/z: 1037.4399, error: −4.9 ppm. (c) Proposed surfactant degradation scheme based on LC−MS results.
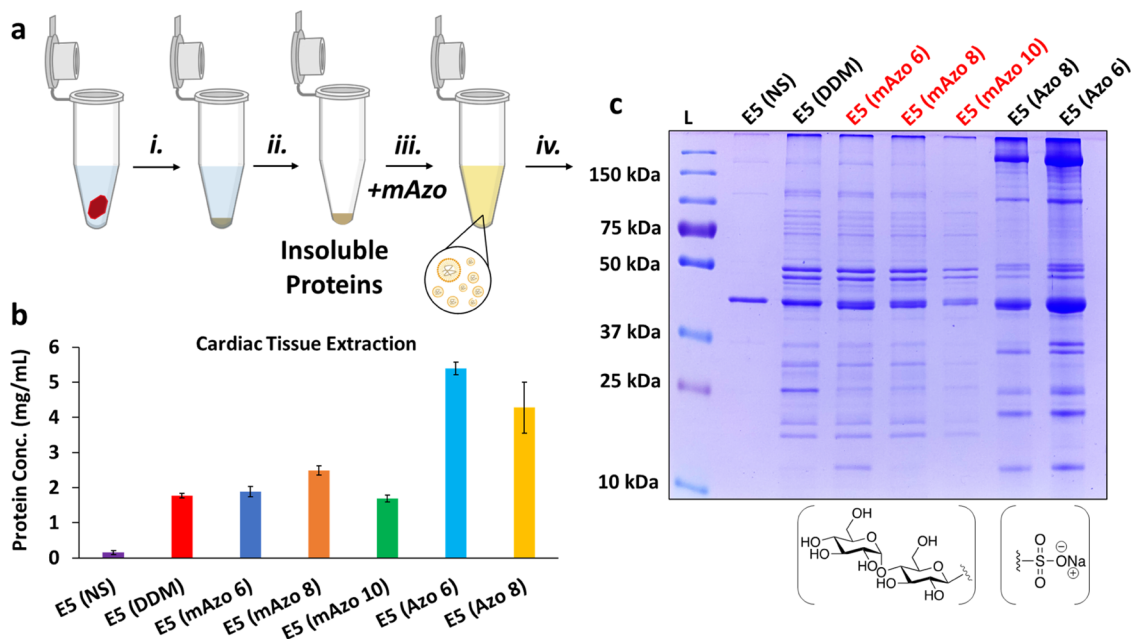
Figure 6. Insoluble protein extraction performance of mAzo surfactants. (a) Tissue extraction workflow: (i) cell lysis and homogenization, (ii) centrifugation and removal of supernatant, (iii) extraction using a surfactant, (iv) sample analysis of soluble proteins via Bradford assay or SDS-PAGE. (b) Bradford assay results from triplicate insoluble protein extracts using either no surfactant (NS), DDM, mAzo 6, mAzo 8, mAzo 10, Azo 6, or Azo 8. (c) 12% SDS-PAGE of insoluble protein extracts using the same sets of surfactants.

the chromatograms for each surfactant were dominated by one large peak that corresponds to a mixture of surfactant monomer, dimer, and trimer, which are typical association patterns in the gas phase for molecules containing a sugar motif. After photodegradation, two species prevailed in each chromatogram, one of which was consistent with a disulfide compound formed from the oxidation of two thiomaltose fragments (Y) and eluted earlier in the gradient relative to the intact surfactant (X; Figure 5a). The second compound, Z, eluted close to the original surfactant peak and had a mass that corresponds to a compound consisting of a maltose head group and an alkylbenzene tail that were linked through a thioether bond. This amphiphilic product is likely to alter surface tension, which explains the observed decrease in surface tension as a function of surfactant concentration even after irradiation (Figure 4a−c). These photodegradation products were consistent across mAzo surfactants with different surfactant chain lengths (Figures S9 and S10).

Based on these results, we propose that the surfactant degrades upon irradiation by two pathways as illustrated in Figure 5c. The first is the traditional (and original anticipated) pathway wherein the surfactant undergoes homolytic cleavage to form maltose (which in turn forms a disulfide bond with another free molecule of thiomaltose yielding Y), phenol, and alkylbenzene byproducts. We note that the phenolic and benzene-derived degradation products in pathway 1 were not observed likely because of the poor ionization efficiency of these species using electrospray ionization (ESI)-MS analysis. The amphiphilic product Z from pathway 2 forms because of the recombination of thiomaltose and alkylbenzyl radicals (Figure S11). Interestingly, when surfactant solutions were allowed to degrade under nonphotolytic conditions (i.e., allowed to remain in the dark in room temperature water), this amphiphilic product still formed as evidenced by LC−MS (Figure S12), albeit to a lesser extent. The formation of this new product under nonphotolytic conditions could proceed *via* an alternative mechanism (Figure S13). Overall, the formation of a new surfactant (Z) explains the continued decrease in surface tension observed in Figure 4 even after photodegradation.

Finally, we explored the use of the mAzo surfactants for protein extraction, as surfactants are widely used throughout biology to solubilize proteins from cells and tissues.[6,44,45] To examine this property of the mAzo surfactants, heart tissue was homogenized and washed in NH_4HCO_3 extraction and washing buffers to remove water-soluble proteins and obtain an insoluble tissue pellet (Figure 6a). Depleting the soluble species allows us to better evaluate the surfactants' ability to extract challenging, insoluble proteins such as membrane proteins. The pellet was then treated with the mAzo surfactants (1% w/v), DDM (1% w/v), no surfactant (NS), or the Azo surfactants (1% w/v or 0.2% w/v, based on maximum solubility in water), which have been previously shown to facilitate protein extraction (Figure 6b,c).[13] The concentration of surfactants used is in great excess of their CMC to achieve high protein solubilization.[44,46] All steps were performed at 4 °C to prevent surfactant degradation as well as to reduce proteolytic activity and preserve protein integrity. Thus, the mAzo surfactants can serve as a cleavable alternative to common biological surfactants when this functionality is desirable (*e.g.*, detergent exchange).[17,47]

Overall, all extraction conditions using various surfactants, including the mAzo surfactants, show an improved protein extraction efficacy relative to using no surfactant. The Bradford assay results in Figure 6b as well as the SDS-polyacrylamide gel electrophoresis (SDS-PAGE) gel in Figure 6c show that mAzo 8 provides the best protein solubility, while mAzo 6, mAzo 10, and DDM were slightly less effective. The results suggest a chain length of 8 provides the best hydrophilic−lipophilic balance to enable protein solubilization for the mAzo surfactants.

Not surprisingly, anionic surfactants like Azo 6 and Azo 8 appear to be more effective at solubilizing proteins compared to the nonionic surfactants,[6,13,35,45] even though they contain the same hydrophobic and photocleavable components as the mAzo surfactants. Ionic head groups destabilize lipid membranes and denature proteins by disturbing noncovalent interaction (*e.g.*, hydrogen bonding), enabling more effective protein extraction and solubilization relative to surfactants with nonionic head groups.[48,49] Although the mAzos were less efficient than the anionic Azos at extracting membrane proteins in the current study, these surfactants presumably are superior to the original surfactants in stabilizing extracted membrane proteins.[6,8] Therefore, they could be amenable to techniques requiring nondenaturing conditions such as crystallography[7] or native MS.[29,50,51] Moreover, cleavable surfactants are generally useful in proteomics for protein solubilization and then detergent removal before MS analysis[13,15,16,19,30−32,52,53] or in detergent exchange before biophysical characterization.[17,47]

■ CONCLUSIONS

We have successfully synthesized and characterized a new family of nonionic photocleavable surfactants (mAzo) derived from maltose, azo-sulfide benzenelinker, and a variable hydrophobic alkyl chain. Surface tension measurements, dynamic light scattering, and transmission electron microscopy show that these mAzo surfactants are able to form supramolecular assemblies. UV−visible spectroscopy shows the rapid photodegradation of the mAzo surfactants, and surface tension measurements of the whole post-degradation solutions suggest an unexpected degradation pathway. LC−MS studies of the photodegradation products reveal that the mAzo surfactants could undergo a recombination event after nitrogen expulsion to nonquantitatively form another photo-stable surfactant. Moreover, we have demonstrated that these surfactants are capable of solubilizing proteins in a comparable way to a commercially available nonionic surfactant analogue (DDM), which is widely used for protein purification and crystallography.[7] Despite the complexity of their photo-degradation processes, these new nonionic cleavable mAzo surfactants provide another set of tools for the applications of mild and switchable surfactants in chemical synthesis, green chemistry, drug delivery, characterization of insoluble bio-molecules, and more.

■ ASSOCIATED CONTENT

ⓈSupporting Information

The Supporting Information is available free of charge at https://pubs.acs.org/doi/10.1021/acs.langmuir.2c02820.

> ^1H NMR spectra of 1-isothiouronium-β-D-maltose heptaacetate fluoride; ^1H NMR spectra of 1-thio-β-D-maltose heptaacetate; ^1H NMR spectra of 1-thio-β-D-maltose potassium salt; ^1H NMR spectra of mAzo 6; ^1H NMR of mAzo 8; ^1H NMR spectra of mAzo 10; solution stability determination of mAzo 6, mAzo 8, and mAzo

10 at room temperature and 4 °C; surface tension measurements for replicate CMC trials for mAzo 6, mAzo 8, and mAzo 10; dynamic light scattering curves for mAzo 6, mAzo 8, and mAzo 10 after photodegradation; EICs of photodegradation products from mAzo 8 and mAzo 10; proposed photodegradation mechanism; EICs of thermal degradation products from mAzo 6, mAzo 8, and mAzo 10; proposed thermal degradation mechanism; and particle size, standard deviation, and PDI for triplicate DLS trials before photodegradation (PDF)

■ AUTHOR INFORMATION

Corresponding Authors

    Kyle A. Brown − *Department of Chemistry, University of Wisconsin−Madison, Madison, Wisconsin 53706, United States; Department of Surgery, University of Wisconsin−Madison, Madison, Wisconsin 53706, United States;* ⊙ orcid.org/0000-0003-1255-9146; Email: kbrown33@wisc.edu

    Song Jin − *Department of Chemistry, University of Wisconsin−Madison, Madison, Wisconsin 53706, United States;* ⊙ orcid.org/0000-0001-8693-7010; Email: jin@chem.wisc.edu

Authors

    Morgan K. Gugger − *Department of Chemistry, University of Wisconsin−Madison, Madison, Wisconsin 53706, United States*

    David S. Roberts − *Department of Chemistry, University of Wisconsin−Madison, Madison, Wisconsin 53706, United States;* ⊙ orcid.org/0000-0002-0478-4987

    David Moreno − *Department of Chemistry, University of Wisconsin−Madison, Madison, Wisconsin 53706, United States*

    Pil Seok Chae − *Department of Bionano Engineering, Hanyang University, Ansan 15588, South Korea;* ⊙ orcid.org/0000-0003-1799-3304

    Ying Ge − *Department of Chemistry, University of Wisconsin−Madison, Madison, Wisconsin 53706, United States; Department of Cell and Regenerative Biology and Human Proteomics Program, School of Medicine and Public Health, University of Wisconsin−Madison, Madison, Wisconsin 53705, United States;* ⊙ orcid.org/0000-0001-5211-6812

Complete contact information is available at:
https://pubs.acs.org/10.1021/acs.langmuir.2c02820

Author Contributions

#K.A.B. and M.K.G. contributed equally to this work.

Notes

The authors declare no competing financial interest.

■ ACKNOWLEDGMENTS

■ REFERENCES

(1) Chowdhury, S.; Shrivastava, S.; Kakati, A.; Sangwai, J. S. Comprehensive Review on the Role of Surfactants in the Chemical Enhanced Oil Recovery Process. *Ind. Eng. Chem. Res.* **2022**, *61*, 21−64.

(2) De, S.; Malik, S.; Ghosh, A.; Saha, R.; Saha, B. A review on natural surfactants. *RSC Adv.* **2015**, *5*, 65757−65767.

(3) Song, T.; Gao, F.; Guo, S.; Zhang, Y.; Li, S.; You, H.; Du, Y. A review of the role and mechanism of surfactants in the morphology control of metal nanoparticles. *Nanoscale* **2021**, *13*, 3895−3910.

(4) Raffa, P.; Wever, D. A. Z.; Picchioni, F.; Broekhuis, A. A. Polymeric Surfactants: Synthesis, Properties, and Links to Applications. *Chem. Rev.* **2015**, *115*, 8504−8563.

(5) Menger, F. M.; Mbadugha, B. N. A. Gemini Surfactants with a Disaccharide Spacer. *J. Am. Chem. Soc.* **2001**, *123*, 875−885.

(6) Lee, H. J.; Lee, H. S.; Youn, T.; Byrne, B.; Chae, P. S. Impact of novel detergents on membrane protein studies. *Chem* **2022**, *8*, 980−1013.

(7) Stetsenko, A.; Guskov, A. An Overview of the Top Ten Detergents Used for Membrane Protein Crystallization. *Crystals* **2017**, *7*, No. 197.

(8) Rasmussen, S. G. F.; Devree, B. T.; Zou, Y.; Kruse, A. C.; Chung, K. Y.; Kobilka, T. S.; Thian, F. S.; Chae, P. S.; Pardon, E.; Calinski, D.; et al. Crystal structure of the *β* 2 adrenergic receptor-Gs protein complex. *Nature* **2011**, *477*, 549−557.

(9) Alpes, H.; Apell, H. J.; Knoll, G.; Plattner, H.; Riek, R. Reconstitution of Na+/K+-ATPase into phosphatidylcholine vesicles by dialysis of nonionic alkyl maltoside detergents. *Biochim. Biophys. Acta, Biomembr.* **1988**, *946*, 379−388.

(10) Wan, Y.; Shi, Y.; Zhao, D. Designed synthesis of mesoporous solids via nonionic-surfactant-templating approach. *Chem. Commun.* **2007**, 897−926.

(11) da Silva, M. A.; Dreiss, C. A. Unusual Surfactants. In *Wormlike Micelles: Advances in Systems, Characterisation and Applications*; The Royal Society of Chemistry, 2017; pp 63−102.

(12) Hellberg, P.-E.; Bergström, K.; Holmberg, K. Cleavable surfactants. *J. Surfactants Deterg.* **2000**, *3*, 81−91.

(13) Brown, K. A.; Chen, B.; Guardado-Alvarez, T. M.; Lin, Z.; Hwang, L.; Ayaz-Guner, S.; Jin, S.; Ge, Y. A photocleavable surfactant for top-down proteomics. *Nat. Methods* **2019**, *16*, 417−420.

(14) Chang, Y.-H.; Gregorich, Z. R.; Chen, A. J.; Hwang, L.; Guner, H.; Yu, D.; Zhang, J.; Ge, Y. New Mass-Spectrometry-Compatible Degradable Surfactant for Tissue Proteomics. *J. Proteome Res.* **2015**, *14*, 1587−1599.

(15) Saveliev, S. V.; Woodroofe, C. C.; Sabat, G.; Adams, C. M.; Klaubert, D.; Wood, K.; Urh, M. Mass Spectrometry Compatible Surfactant for Optimized In-Gel Protein Digestion. *Anal. Chem.* **2013**, *85*, 907−914.

(16) Yu, Y. Q.; Gilar, M.; Lee, P. J.; Bouvier, E. S.; Gebler, J. C. Enzyme-friendly, mass spectrometry-compatible surfactant for in-solution enzymatic digestion of proteins. *Anal. Chem.* **2003**, *75*, 6023−6028.

(17) Liu, L.; Zhu, Z.; Zhou, F.; Xue, D.; Hu, T.; Luo, W.; Qiu, Y.; Wu, D.; Zhao, F.; Le, Z.; Tao, H. Catalytically Cleavable Detergent for Membrane Protein Studies. *ACS Omega* **2021**, *6*, 21087−21093.

(18) Hwang, L.; Guardado-Alvarez, T. M.; Ayaz-Gunner, S.; Ge, Y.; Jin, S. A Family of Photolabile Nitroveratryl-Based Surfactants That Self-Assemble into Photodegradable Supramolecular Structures. *Langmuir* **2016**, *32*, 3963−3969.

(19) Norris, J. L.; Hangauer, M. J.; Porter, N. A.; Caprioli, R. M. Nonacid cleavable detergents applied to MALDI mass spectrometry profiling of whole cells. *J. Mass Spectrom.* **2005**, *40*, 1319−1326.

(20) Epstein, W. W.; Jones, D. S.; Bruenger, E.; Rilling, H. C. The synthesis of a photolabile detergent and its use in the isolation and characterization of protein. *Anal. Biochem.* **1982**, *119*, 304−312.

(21) Nuyken, O.; Meindl, K.; Wokaun, A.; Mezger, T. Photolabile surfactants based on the diazosulphonate group 2. 4-(Acyloxy)-benzenediazosulphonates and 4-(acylamino)-

benzenediazosulphonates. *J. Photochem. Photobiol., A* **1995**, *85*, 291−298.

(22) Jaeger, D. A.; Reddy, V. B.; Bohle, D. S. Cleavable double-chain surfactant Co(III) complexes. *Tetrahedron Lett.* **1999**, *40*, 649−652.

(23) Dunkin, I. R.; Gittinger, A.; Sherrington, D. C.; Whittaker, P. Synthesis, characterization and applications of azo-containing photo-destructible surfactants. *J. Chem. Soc., Perkin Trans. 2* **1996**, 1837−1842.

(24) Norris, J. L.; Porter, N. A.; Caprioli, R. M. Mass Spectrometry of Intracellular and Membrane Proteins Using Cleavable Detergents. *Anal. Chem.* **2003**, *75*, 6642−6647.

(25) Kakiyama, T.; Usui, K.; Tomizaki, K.-y.; Mie, M.; Kobatake, E.; Mihara, H. A peptide release system using a photo-cleavable linker in a cell array format for cell-toxicity analysis. *Polym. J.* **2013**, *45*, 535−539.

(26) Mezger, T.; Nuyken, O.; Meindl, K.; Wokaun, A. Light decomposable emulsifiers: application of alkyl-substituted aromatic azosulfonates in emulsion polymerization. *Prog. Org. Coat.* **1996**, *29*, 147−157.

(27) Nuyken, O.; Voit, B. The photoactive diazosulfonate group and its role in polymer chemistry. *Macromol. Chem. Phys.* **1997**, *198*, 2337−2372.

(28) Kim, M. S.; Diamond, S. L. Photocleavage of o-nitrobenzyl ether derivatives for rapid biomedical release applications. *Bioorg. Med. Chem. Lett.* **2006**, *16*, 4007−4010.

(29) Urner, L. H.; Schulze, M.; Maier, Y. B.; Hoffmann, W.; Warnke, S.; Liko, I.; Folmert, K.; Manz, C.; Robinson, C. V.; Haag, R.; Pagel, K. A new azobenzene-based design strategy for detergents in membrane protein research. *Chem. Sci.* **2020**, *11*, 3538−3546.

(30) Brown, K. A.; Tucholski, T.; Eken, C.; Knott, S.; Zhu, Y.; Jin, S.; Ge, Y. High-throughput Proteomics Enabled by a Photocleavable Surfactant. *Angew. Chem., Int. Ed.* **2020**, *59*, 8406−8410.

(31) Knott, S. J.; Brown, K. A.; Josyer, H.; Carr, A.; Inman, D.; Jin, S.; Friedl, A.; Ponik, S. M.; Ge, Y. Photocleavable Surfactant-Enabled Extracellular Matrix Proteomics. *Anal. Chem.* **2020**, *92*, 15693−15698.

(32) Buck, K. M.; Roberts, D. S.; Aballo, T. J.; Inman, D. R.; Jin, S.; Ponik, S.; Brown, K. A.; Ge, Y. One-Pot Exosome Proteomics Enabled by a Photocleavable Surfactant. *Anal. Chem.* **2022**, *94*, 7164−7168.

(33) Aballo, T. J.; Roberts, D. S.; Melby, J. A.; Buck, K. M.; Brown, K. A.; Ge, Y. Ultrafast and Reproducible Proteomics from Small Amounts of Heart Tissue Enabled by Azo and timsTOF Pro. *J. Proteome Res.* **2021**, *20*, 4203−4211.

(34) Brown, G. M.; Dubreuil, P.; Ichhaporia, F. M.; Desnoyers, J. E. Synthesis and properties of some α-D-alkyl glucosides and manno-sides: apparent molal volumes and solubilization of nitrobenzene in water at 25 °C. *Can. J. Chem.* **1970**, *48*, 2525−2531.

(35) Chae, P. S.; Rasmussen, S. G. F.; Rana, R. R.; Gotfryd, K.; Chandra, R.; Goren, M. A.; Kruse, A. C.; Nurva, S.; Loland, C. J.; Pierre, Y.; et al. Maltose−neopentyl glycol (MNG) amphiphiles for solubilization, stabilization and crystallization of membrane proteins. *Nat. Methods* **2010**, *7*, 1003−1008.

(36) Bradley, M.; Vincent, B.; Warren, N.; Eastoe, J.; Vesperinas, A. Photoresponsive Surfactants in Microgel Dispersions. *Langmuir* **2006**, *22*, 101−105.

(37) Ibatullin, F. M.; Shabalin, K. A.; Jänis, J. V.; Shavva, A. G. Reaction of 1,2-trans-glycosyl acetates with thiourea: a new entry to 1-thiosugars. *Tetrahedron Lett.* **2003**, *44*, 7961−7964.

(38) Doyle, L. M.; O'Sullivan, S.; Di Salvo, C.; McKinney, M.; McArdle, P.; Murphy, P. V. Stereoselective Epimerizations of Glycosyl Thiols. *Org. Lett.* **2017**, *19*, 5802−5805.

(39) McElhanon, J. R.; Zifer, T.; Kline, S. R.; Wheeler, D. R.; Loy, D. A.; Jamison, G. M.; Long, T. M.; Rahimian, K.; Simmons, B. A. Thermally Cleavable Surfactants Based on Furan−Maleimide Diels−Alder Adducts. *Langmuir* **2005**, *21*, 3259−3266.

(40) Maibaum, L.; Dinner, A. R.; Chandler, D. Micelle Formation and the Hydrophobic Effect. *J. Phys. Chem. B* **2004**, *108*, 6778−6781.

(41) Shin, J. Y.; Abbott, N. L. Using Light to Control Dynamic Surface Tensions of Aqueous Solutions of Water Soluble Surfactants. *Langmuir* **1999**, *15*, 4404−4410.

(42) Aguilar, Z. P. Types of Nanomaterials and Corresponding Methods of Synthesis. In *Nanomaterials for Medical Applications*; Aguilar, Z. P., Ed.; Elsevier, 2013; pp 33−82.

(43) Kwan, T. O. C.; Reis, R.; Siligardi, G.; Hussain, R.; Cheruvara, H.; Moraes, I. Selection of Biophysical Methods for Characterisation of Membrane Proteins. *Int. J. Mol. Sci.* **2019**, *20*, No. 2605.

(44) Hussain, H.; Du, Y.; Scull, N. J.; Mortensen, J. S.; Tarrasch, J.; Bae, H. E.; Loland, C. J.; Byrne, B.; Kobilka, B. K.; Chae, P. S. Accessible Mannitol-Based Amphiphiles (MNAs) for Membrane Protein Solubilisation and Stabilisation. *Chem. - Eur. J.* **2016**, *22*, 7068−7073.

(45) Speers, A. E.; Wu, C. C. Proteomics of integral membrane proteins–theory and application. *Chem. Rev.* **2007**, *107*, 3687−3714.

(46) Ohlendieck, K. Purification of Membrane Proteins. In *Protein Purification Protocols*; Cutler, P., Ed.; Humana Press, 2004; pp 301−308.

(47) Xue, D.; Wang, J.; Song, X.; Wang, W.; Hu, T.; Ye, L.; Liu, Y.; Zhou, Q.; Zhou, F.; Jiang, Z.-X.; et al. A Chemical Strategy for Amphiphile Replacement in Membrane Protein Research. *Langmuir* **2019**, *35*, 4319−4327.

(48) Rabilloud, T. Protein Solubility in Two-Dimensional Electro-phoresis. In *The Protein Protocols Handbook*; Walker, J. M., Ed.; Humana Press, 2009; pp 73−84.

(49) Seddon, A. M.; Curnow, P.; Booth, P. J. Membrane proteins, lipids and detergents: not just a soap opera. *Biochim. Biophys. Acta, Biomembr.* **2004**, *1666*, 105−117.

(50) Keener, J. E.; Zhang, G.; Marty, M. T. Native Mass Spectrometry of Membrane Proteins. *Anal. Chem.* **2021**, *93*, 583−597.

(51) Urner, L. H.; Liko, I.; Yen, H. Y.; Hoi, K. K.; Bolla, J. R.; Gault, J.; Almeida, F. G.; Schweder, M. P.; Shutin, D.; Ehrmann, S.; et al. Modular detergents tailor the purification and structural analysis of membrane proteins including G-protein coupled receptors. *Nat. Commun.* **2020**, *11*, No. 564.

(52) Chen, E. I.; Cociorva, D.; Norris, J. L.; Yates, J. R. Optimization of Mass Spectrometry Compatible Surfactants for Shotgun Proteomics. *J. Proteome Res.* **2007**, *6*, 2529−2538.

(53) Brown, K. A.; Gugger, M. K.; Yu, Z.; Moreno, D.; Jin, S.; Ge, Y. Nonionic, Cleavable Surfactant for Top-Down Proteomics. *Anal. Chem.* **2023**, DOI: 10.1021/acs.analchem.2c03916.